Molecular Therapy
Methods & Clinical Development
Original Article

Efficacy of a Bicistronic Vector for Correction of Sandhoff Disease in a Mouse Model

Evan Woodley,[1] Karlaina J.L. Osmon,[2] Patrick Thompson,[1] Christopher Richmond,[1] Zhilin Chen,[3] Steven J. Gray,[4,5] and Jagdeep S. Walia[1,2,3]

[1]Department of Biomedical and Molecular Sciences, Queen's University, Kingston, ON, Canada; [2]Centre for Neuroscience Studies, Queen's University, Kingston, ON, Canada; [3]Medical Genetics/Departments of Pediatrics, Queen's University, Kingston, ON, Canada; [4]Gene Therapy Center, University of North Carolina, Chapel Hill, NC, USA; [5]Department of Pediatrics; UT Southwestern Medical Center, Dallas, TX, USA

G_{M2} gangliosidoses are a family of severe neurodegenerative disorders resulting from a deficiency in the β-hexosaminidase A enzyme. These disorders include Tay-Sachs disease and Sandhoff disease, caused by mutations in the *HEXA* gene and *HEXB* gene, respectively. The *HEXA* and *HEXB* genes are required to produce the α and β subunits of the β-hexosaminidase A enzyme, respectively. Using a Sandhoff disease mouse model, we tested for the first time the potential of a comparatively lower dose (2.04×10^{13} vg/kg) of systemically delivered single-stranded adeno-associated virus 9 expressing both human *HEXB* and human *HEXA* cDNA under the control of a single promoter with a P2A-linked bicistronic vector design to correct the neurological phenotype. A bicistronic design allows maximal overexpression and secretion of the Hex A enzyme. Neonatal mice were injected with either this ssAAV9-HexB-P2A-HexA vector or a vehicle solution via the superficial temporal vein. An increase in survival of 56% compared with vehicle-injected controls and biochemical analysis of the brain tissue and serum revealed an increase in enzyme activity and a decrease in brain G_{M2} ganglioside buildup. This is a proof-of-concept study showing the "correction efficacy" of a bicistronic AAV9 vector delivered intravenously for G_{M2} gangliosidoses. Further studies with higher doses are warranted.

INTRODUCTION

G_{M2} gangliosidoses are a family of fatal, autosomal recessive, lysosomal storage disorders (LSDs) caused by accumulation of the G_{M2} ganglioside in the lysosomes of cells, primarily within the CNS. The cause of this buildup is a deficiency in the β-hexosaminidase A enzyme (Hex A), which is responsible for hydrolysis of the G_{M2} ganglioside. The Hex A enzyme is a heterodimer composed of 2 subunits: β-hexosaminidase α (encoded in humans by the *HEXA* gene) and β-hexosaminidase β (encoded in humans by the *HEXB* gene). G_{M2} gangliosidosis caused by a mutation of the *HEXA* gene is termed Tay-Sachs disease (TSD), whereas the phenotype caused by a mutation of the *HEXB* gene is termed as Sandhoff disease (SD). The resulting substrate buildup is focused in the CNS and results in inflammation, cell death, and neurodegeneration through a poorly understood cascade of events.[1,2]

In the general population, the carrier frequency of TSD is 1 in 300 but is as high as 1 in 25 in populations of Ashkenazi Jewish descent,[3–6] whereas SD has a carrier rate of about 1 in 278 in the general population;[6–8] however, these rates are also higher in certain founder populations.[9,10] TSD and SD result in clinically indistinguishable phenotypes for which there is no effective treatment.[1,2] In its most common and severe form, the disease is characterized by a complete lack of Hex A activity and is termed infantile-onset. In this case, the children appear normal at birth, followed by rapid neurodegeneration culminating in death before the age of 4.[1,11,12] Hex A enzyme activity levels of 10%–15% of wild-type (WT) Hex A activity, termed the "critical threshold," have been shown to be sufficient to sustain normal metabolism.[13,14]

G_{M2} gangliosidoses and other LSDs make prime targets for gene therapy treatment for a number of reasons. First, LSDs are primarily monogenic disorders that could be cured by improving the expression of a single gene. Additionally, lysosomal enzymes are ubiquitously expressed, resulting in little concern for off-target effects, and overexpression of the enzymes does not seem to be detrimental. Next, lysosomal enzymes, including Hex A, are secreted from transduced cells and can be taken up by neighboring cells to correct their phenotype via the M6PR pathway, making it possible to cure these diseases without the need to transduce every cell.[15,16] Lastly, as already discussed, enzyme activity of approximately 10% of WT levels may result in complete phenotypic absence of the disease.[13,14] Because of this, G_{M2} gangliosidoses have a long history of gene therapy studies, primarily in the SD mouse and feline models that show a significant amount of promise in ameliorating the disease with a one-time curative treatment.

The choice of vector in a gene therapy trial is crucial for the success of the treatment. Recombinant adeno-associated virus (AAV) serotype 9 (AAV9) has been shown to cross the blood-brain barrier (BBB) when

Received 29 September 2018; accepted 23 October 2018;
https://doi.org/10.1016/j.omtm.2018.10.011.

Correspondence: Jagdeep S. Walia, Queen's University, 76 Stuart Street, Armstrong 4, Kingston General Hospital, Kingston, ON K7L 2V7, Canada.
E-mail: jagdeep.walia@kingstonhsc.ca

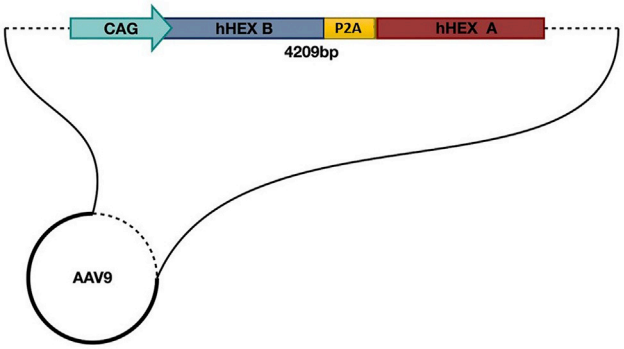

Figure 1. ssAAV9-HexB-P2A-HexA Construct Design

The human *HEXA* and *HEXB* genes were synthesized with a self-cleaving linker, P2A, between them and with a CAG promoter upstream to drive expression. The entire construct was designed between the appropriate AAV inverted terminal repeat (ITR) elements, and an SV40 element was included to promote protein expression in mammalian cells.

introduced intravenously and to preferentially transduce neurons in neonates and astrocytes in adult mice,[17] rats,[18] cats,[19] and non-human primates.[20–23]

In the search for a viable gene therapy treatment for G_{M2} gangliosidoses, *in vitro* experiments were performed. Human *HEXA* cDNA subcloned into an adenoviral plasmid was first used to transfect fibroblasts derived from a patient suffering from TSD in 1996.[24] Further studies showed that delivery of both the *HEXA* gene and the *HEXB* gene is required to achieve maximal overexpression and secretion of the Hex A enzyme above WT levels in transduced cells, resulting in massive secretion throughout the TSD mouse.[24,25] a result also seen in SD mouse fibroblasts.[26] These results suggested that these *in vitro* gene therapy treatments may have success *in vivo*.

The murine model for SD was generated through disruption of the murine *hexb* gene with a neomycin cassette[27–30] and showed near-complete deficiency in the murine Hex A enzyme exhibiting a severe phenotype,[31] typically reaching humane endpoints at 15–17 weeks.[28,29] Feline and ovine models for G_{M2} gangliosidoses are also used in preclinical gene therapy trials.[32]

Preclinical *in vivo* gene therapy studies have been carried out in both the feline and murine disease models. Transduction of *HEXA* and *HEXB* on separate vectors results in sustained and widespread Hex A enzyme activity throughout the CNS following direct injection into the CNS. Inflammation and G_{M2} ganglioside storage are typically decreased, and increases in survival to over a year in mice and return to WT behavioral phenotypes are possible with high doses.[33–41] Successful application of AAV9 systemic (intravenous) treatments for G_{M2} gangliosidoses in mice has been observed using a vector expressing *hexb*[42] and a hybrid hexosaminidase gene, *HEXM*.[43]

Some studies have used single vectors encoding either the α or β subunit to treat TSD or SD successfully, respectively, but emphasized the importance of having both units to make the HexA isoform.[31,42,44] Other studies have utilized multiple vectors carrying the *HEXA* and *HEXB* genes separately to take advantage of the increased enzyme secretion that results from overexpression of both the α and β subunit.[35,38–40] Both of these approaches, however, have major drawbacks compared with a bicistronic vector design carrying both genes in a single vector. Multiple vector treatments must be given at higher doses to see the desired increased expression because both vectors must transduce the same cell to optimally overexpress the Hex A enzyme. Comparatively, a bicistronic vector design may allow a lower, single-vector dose to achieve the same results. Dosages are important when considering the humoral response to the vector, cost of treatment, and risk of insertional oncogenesis events, all of which increase with an increased dose.[45] No systemically injected bicistronic treatment of SD or TSD in an animal model has been reported in the literature to date. Self-cleaving 2A peptides have been used successfully in previous studies, showing its utility as one of the most effective 2A linkers for the cleavage and expression of multicistronic constructs.[46–49]

A proof-of-concept study is presented here examining the therapeutic potential of a bicistronic AAV9-HexBP2A-HexA viral vector administered via a systemic injection. By utilizing a short P2A linker, cDNAs of both the human *HEXA* and *HEXB* genes were packaged into a single stranded AAV9 vector under the same CAG promoter. We hypothesized that this approach should maximize the expression of Hex A enzyme while minimizing the required total AAV dosage for these neonatal injections using a relatively non-invasive systemic administration.

RESULTS

In Vitro Analysis of the HexB-HexA Construct

The HexB-HexA construct was designed as shown in Figure 1 (HexB and HexA denotes the proteins) HEK-HexABKO (ABKO) cells were made to express no hexosaminidase activity as confirmed by PCR sequencing, western blot analysis, and hex activity assays.[50] These ABKO cells were kindly donated by Dr. Don Mahuran (SickKids, Toronto, ON). ABKO cells were transfected via a standard calcium phosphate protocol with a plasmid encoding the same HexB-HexA construct. Following transfection, and diethylaminoethyl (DEAE) separation of hexosaminidase isoforms, transfected cell cultures were observed to be expressing all three isoforms of the hexosaminidase enzyme (Hex B, Hex A, and Hex S) at levels equal to or greater than WT HEK293 cells. Untransfected HexABKO cells showed no hexosaminidase activity. These results are shown in Figure 2A.

To assess the protein expression of the HexB-HexA vector, ABKO cells were transfected with the HexB-HexA construct with Lipofectamine 2000. Transfected cells were then collected and lysed to obtain a protein lysate. Western blot analysis revealed that, unlike ABKO cells, which do not produce any mature HexA or HexB protein, ABKO cells transfected with the HexB-HexA construct did show

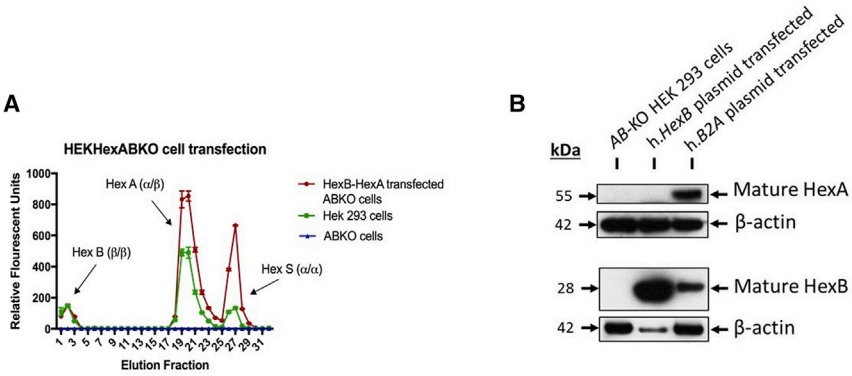

Figure 2. Hexosaminidase Activity and Protein Expression in HEKHexABKO Cells Transfected with the HexB-HexA Construct

(A) MUG substrate was used to assess the hexosaminidase activity of cell lysates following DEAE column separation. ABKO cells showed no hexosaminidase activity above baseline, whereas WT HEK293 cells showed activity of all 3 isoforms of hexosaminidase. Following transfection with HexB-HexA, ABKO cells showed levels of hex activity equal to or greater than the WT HEK293 cells in all eluted fractions. (B) Protein expression analysis was conducted through western blot analysis, probing with anti-HEXA and anti-HEXB antibodies. Un-transfected HEKHexABKO cells showed no mature HexA or HexB expression, whereas ABKO cells transfected with the HexB-HexA construct (h.B2A plasmid) showed mature HexA and HexB expression levels.

mature expression of the HexA and HexB proteins. These results are shown in Figure 2B.

In Vivo Analysis of the HexB-HexA Construct

To evaluate the effectiveness of a single intravenous injection of the HexB-HexA vector, cohorts of 12 SD ($hexb^{-/-}$) mice received either the treatment vector at a low dose of 2.04×10^{13} vector genomes (vg)/kg or a vehicle control administered via the superficial vein on post-natal day 1. Additionally, a control group of 12 Het mice ($hexb^{+/-}$) received a vehicle injection. Six mice from each cohort were euthanized at 16 weeks for biochemical and histological analyses. The remaining six mice provided survival and behavioral data until their endpoint, as indicated by either a 10% body weight loss, inability to right themselves in 10 s, or the study endpoint of 32 weeks.

Effect of HexB-HexA on Survival

HexB-HexA vector delivery had a marked effect on the lifespan, increasing the mean age of survival from 110 ± 6.3 days in untreated SD mice to 170 ± 8.0 days ($p = 0.0002$). Figure 3 shows a comparison of the HexB-HexA treatment against that of vehicle-injected Het and SD mice.

Effect of HexB-HexA on Motor Activity

Disease progression in SD mice was measured non-invasively through a series of behavioral tests. Performance in the open field test (OFT) has been shown to correlate with disease progression.[42,43] Additionally, measurements of the righting reflex and mesh test scores are used to assess quality of life and mouse strength in disease models.[51,52]

Testing at 14 and 16 weeks showed significant improvement in OFT time moving with HexB-HexA treatment compared with SD controls. At 14 weeks, untreated SD mice had a mean time moving of 55.5 ± 8.7 s, and HexB-HexA-treated mice scored a mean of 114.7 ± 21.1 s ($p < 0.001$). At 16 weeks, the two groups had a mean time moving of 40.7 ± 6.7 s and 115.3 ± 22.0 s, respectively ($p < 0.001$). At 24 weeks, as HexB-HexA treated mice neared their eventual endpoints, they performed significantly worse than the Het control mice for the first time, with a mean time moving of 37 ± 10.2 s and 85.5 ± 15.2 s ($p = 0.0025$), respectively. Figure 4 illustrates the comparison of OFT time moving between all cohorts.

HexB-HexA-treated SD mice (n = 6) had no delay in righting reflex until 22 weeks, whereas all SD controls (n = 6) reached the maximum score of 10 s between the ages of 14 and 17 weeks. This represented a significant delay in the onset of a delayed righting reflex. Untreated Het mice had no delay in righting reflex until the study endpoint of 32 weeks.

In the mesh test, HexB-HexA-treated mice (n = 6) and Het controls (n = 6) performed significantly better than untreated SD controls (n = 6). At 16 weeks, HexB-HexA-treated mice had a mean score of 60 s, the maximum possible, whereas untreated SD mice averaged 24.8 ± 13.7 s. HexB-HexA-treated SD mice performed similar to Het controls until 24 weeks, at which point they scored a mean time of 27.7 ± 13.9 s ($p = 0.0002$), whereas Het controls maintained a perfect 60-s average.

Effect of HexB-HexA on G_{M2} Ganglioside Storage

At the 16-week time point, 6 mice receiving each therapy were sacrificed, and their tissue was harvested for biochemical and histological analyses according to the plan shown in Figure 5. To assess G_{M2} ganglioside storage in the CNS, high-performance thin-layer chromatography was used to visualize and separate gangliosides. The G_{M2} ganglioside was found to be undetectable in Het control mice but was found at relatively high levels in SD control mice, where approximately 37% of the isolated gangliosides were G_{M2} gangliosides. In comparison, HexB-HexA-treated SD mice had a significantly reduced amount of G_{M2} ganglioside, making up only 25% of total isolated gangliosides ($p < 0.0001$). Ganglioside storage assay results are shown in Figures 6A and 6B.

Effect of HexB-HexA on Hexosaminidase Activity

Consistent with the reduced G_{M2} ganglioside levels in HexB-HexA-treated SD mice, we expected an increase in Hex A activity in the CNS. Assessment of the 16-week midbrains for Hex A activity

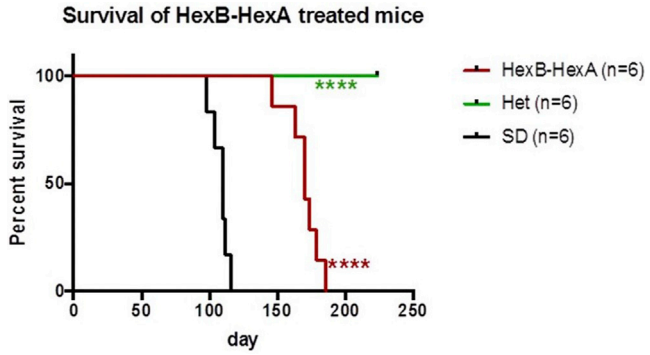

Figure 3. Kaplan-Meier Survival Curve of the AAV-HexB-HexA and Drug-Treated Groups

Shown is survival of mice over 32 weeks. Each point represents the percentage of mice surviving at that time. AAV-HexB-HexA treated-mice survived to a mean of 170 days, ranging from 146 to 186 days (n = 6). This extension in survival is significant compared with the untreated vehicle-injected SD mice with a mean of 110 days (p = 0.0002). All Het mice reached the study endpoint of 224 days. *p < 0.05, **p < 0.01, ***p < 0.001, ****p < 0.0001.

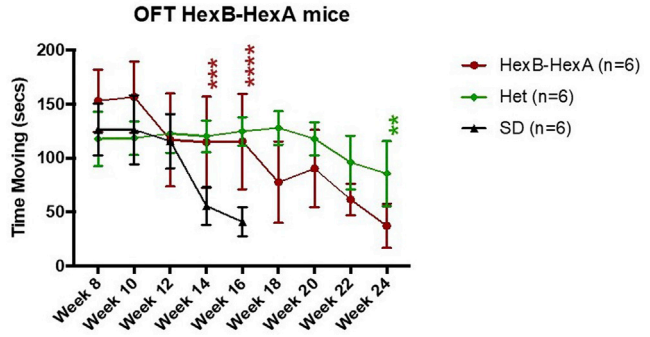

Figure 4. Open Field Test Behavioral Analysis of AAV HexB-HexA and Drug-Treated Mice

Shown is time moving during the 5-min open field test. Each point represents the mean time moving measured on a bi-weekly basis beginning at week 8. HexB-HexA-treated mice (n = 6) had a significantly higher mean time moving at 14 and 16 weeks of age compared with SD controls (n = 6). Het mice (n = 6) performed no better than HexB-HexA-treated SD mice until 24 weeks. *p < 0.05, **p < 0.01, ***p < 0.001, ****p < 0.0001.

did show a consistent increase in the breakdown of 4-methylumbelliferyl-7-6-sulfo-2-acetamido-2-deoxy-β-D-glucopyranoside (4-MUGS); however, this increase was found to be not significant. These results are shown in Figure 6C.

Serum samples that were taken throughout the study allowed us to assess hexosaminidase activity levels prior to the 16-week endpoints. Samples taken from 8-week-old mice showed a significant increase in hexosaminidase activity in HexB-HexA-treated mice (n = 6) compared with untreated SD controls (n = 6), as indicated by the MUGS assay (p = 0.0045; Figure 6D). Additionally, serum was assessed for MUG activity following DEAE separation of hexosaminidase isoforms. HexB-HexA-treated mice were observed to be expressing both Hex B and Hex A activity, along with some possible Hex S activity, at levels much higher than untreated SD controls but still lower than untreated Het controls (Figure 6E).

Histology

Paraffin-embedded MB sections of 16-week-old mice were cut and mounted on positively charged slides. Sections were then stained with the KM966 anti-G_{M2} ganglioside antibody, followed by visualization with a biotinylated secondary antibody and DAB staining protocol. A comparison of staining patterns between untreated SD mice and those that received HexB-HexA treatment showed a pattern of decreased G_{M2} ganglioside buildup in the MB sections. Untreated Het mice revealed no positive staining for the G_{M2} ganglioside. Representative sections are shown in Figure 7.

Vector Biodistribution

The copy number of the HexB-HexA vector was assessed through qPCR analysis and is presented as number of viral genomes per mouse genome, as depicted in Figure 8. We observed a relatively uniform distribution of the vector across the brain and spinal cord areas. There were also relatively high levels of the HexB-HexA vector seen in the heart and liver, which is consistent with previous reports.[21,53]

DISCUSSION

Our study demonstrates, for the first time, the therapeutic potential of the ssAAV9-HexB-P2A-HexA vector, showing both *in vivo* and *in vitro* expression of the α and β subunit and subsequent formation of active Hex A enzyme. As a result, a single systemic dose of the vector in neonatal mice was able to confer extension of lifespan and improvement in behavioral tests.

First we observed that our vector construct produced mature and functional Hex A enzyme from the encoded β and α subunit in the ABKO cell line at levels equal to or greater than those of WT HEK293 cells. This *in vitro* expression, confirmed by western blot and DEAE assays, demonstrates that both the β and α subunits are fully formed in sufficient quantities, indicating the success of the P2A linker, which has been shown to have between 90%–100% cleavage efficiency.[46–49]

Next, this vector was assessed *in vivo* at a relatively low dose in the SD animal model. The treated SD mice lived significantly longer than the untreated controls and performed significantly better on the OFT at age 14 and 16 weeks, the mesh test at 16 weeks, and the righting reflex at age 14 and 16 weeks. These results are consistent with similar studies.[42–44,51] Overall, the treated cohort showed a delay in the onset of behavioral symptoms of the disease from approximately 14 weeks to 22 weeks of age, when they began to score below the Het controls, indicating that the treatment was effective in increasing the Hex A activity and decreasing the G_{M2} ganglioside storage to a clinically significant degree in the CNS. We did note that both heterozygotes and treated SD mice decreased performance with time, which is likely due to lack of novelty (with frequent testing) and increasing weight with time.

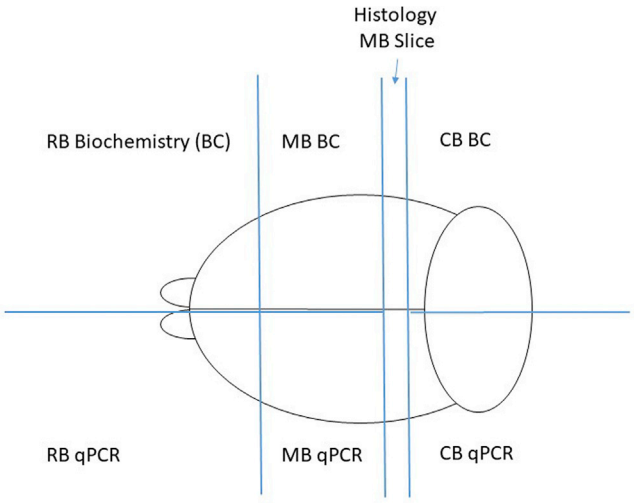

Figure 5. Brain Sectioning

After extraction, the brain was roughly divided into the rostral brain (RB), middle brain (MB), and caudal brain (CB) sections. A 2-mm portion of the midbrain was extracted for histological processing. The remaining RB, MB, and CB slices were then halved, and each half was stored for further qPCR or biochemical analysis.

Biochemical analysis revealed a consistent but non-significant increase in hexosaminidase activity in MB samples of 16-week-old treated mice, whereas a significant increase in Hex A activity was observed in 8-week serum in HexB-HexA-treated mice compared with untreated SD controls. These results suggest that there was a small increase in Hex A activity following treatment that either disappeared over time or was more difficult to detect in the CNS. Ganglioside accumulation was, however, significantly decreased in mice treated with HexB-HexA compared with SD controls, as measured by both the ganglioside extraction assay and histological analysis of the mouse MB. However, even with treatment, all SD mice still showed significant and detectable levels of the G_{M2} ganglioside, whereas Het controls had undetectable levels throughout. These results, taken together, suggest that HexB-HexA treatment resulted in an increase in Hex A activity within the CNS to a level above that of SD controls but still below the critical threshold.

The bicistronic vector treatment approach demonstrates a number of advantages over previous treatments. The bicistronic vector design allows formation of the Hex A enzyme from subunits that are expressed in equal amounts in the same transfected cells compared with approaches that supply only one subunit and are limited by the endogenous subunit or that use two vectors and require significantly higher doses to ensure that the same cells are transfected. Additionally, by utilizing the AAV9 vector, this approach does not require direct intraparenchymal injection into the CNS. As a result, the current study provides a treatment approach that is less invasive but remains effective at lower doses than in most previous approaches.[15,25,33–37,41–44,54]

Assessment of the potential immunogenicity of any gene therapy treatment is necessary to fully evaluate the effect of the treatment construct and viral vector *in vivo*. The HexA-HexB construct was specifically designed to have reduced immunogenicity compared with novel hybrid genes. Although use of the P2A linker brings amino acid residues being added to the C terminus of the beta subunit and a single proline being added to the N terminus of the alpha subunit, it has been shown that such a change has not resulted in any significant immune response.[55] In the current study, the additional amino acids have not interfered with the function of the HEXA enzyme, but future studies should assess their immunological effect.

There were clear limitations in our study. The first one was that our conservative dose was too low for a curative expectation, but it was a proof-of-concept study testing the short-term efficacy *in vivo*, and we succeeded in identifying the significant potential of this vector. The observed increase in survival indicates that the enzyme levels neared the critical threshold enough to change the course of the disease. Further studies are warranted and are being carried out with different higher doses. Slightly higher doses of this viral vector may be enough to completely ameliorate the disease throughout the body. These expected improvements should be investigated through treatment of SD mice, and any results will likely extrapolate to TSD animal models and to higher organisms. This proof-of-concept study provides the foundation for a translatable global treatment for both TSD and SD.

MATERIALS AND METHODS

Animal Models

The SD mice were obtained from The Jackson Laboratory and maintained on a 12-hr light cycle from 7 a.m. to 7 p.m. All experimental protocols and procedures were performed in accordance with the Canadian Council on Animal Care and were approved by the Queen's University Animal Care Committee.

Plasmid and Vector Preparations

The HexB-HexA sequence includes the cDNA of the human *HexB* gene and the human *HexA* gene linked by a P2A self-cleaving peptide under control of the CAG promoter, as shown in Figure 1. BioBasics (Markham, Ontario) synthesized the 4,830-bp construct into a plasmid. The ssAAV9 viral vectors were produced as described previously in Dr. Steven Gray's laboratory at the University of North Carolina[56] from this plasmid.

Injections

Neonatal mice received injections of the HexB-HexA vector or a vehicle control through the superficial temporal vein on day 0–1, as described previously.[42,43] Treated mice received an injection of 2.04×10^{10} vg/mouse in a volume of 50 μL of PBS with 350 nM NaCl and 5% sorbitol (vehicle) using a 30G needle. Untreated control mice received the same vehicle without the vector.

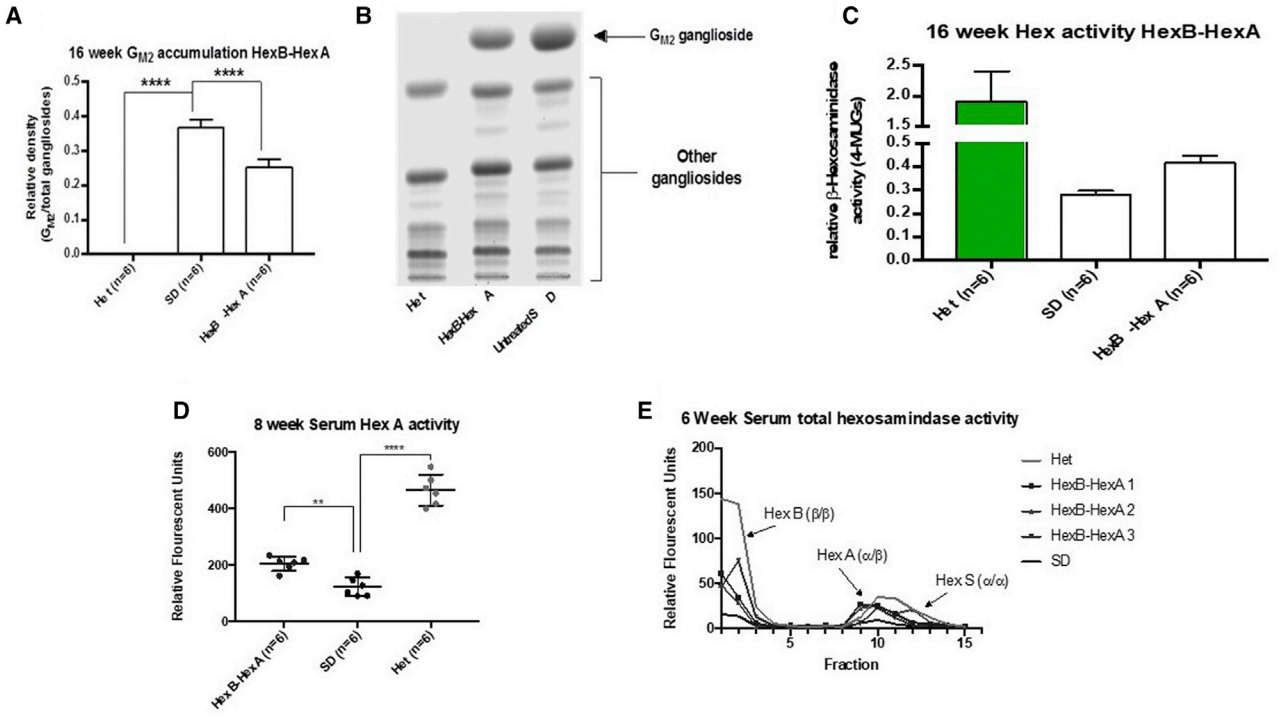

Figure 6. Biochemical Analysis of the HexB-HexA Treatment

(A) Ganglioside storage analysis. Shown is densitometry-based quantification of G_{M2} ganglioside storage in the midbrain. HexB-HexA-treated mice (n = 6) showed a significantly lower proportion of G_{M2} ganglioside than SD controls (n = 6). Het controls showed no accumulation of the G_{M2} ganglioside. (B) Analysis of ganglioside content. Gangliosides isolated from frozen brains as well as standards were separated by high performance thin-layer chromatography (HPTLC) and detected with orcinol. Samples from brains of each cohort were examined. Representative samples are shown here; changes in the G_{M2} ganglioside band can be observed. (C) Analysis of Hex A activity by MUGS assay. No significant alterations in enzyme activity were observed in the treatment group compared with SD controls. (D) Serum collected at 8 weeks was assayed for Hex A activity using MUG substrate. HexB-HexA-treated SD mice (n = 6) showed significantly increased Hex A activity compared with SD controls (n = 6), as indicated by an increased breakdown of the substrate, resulting in an increased fluorescent signal ($p = 0.0045$). (E) Serum collected at 6 weeks was processed to separate hexosaminidase isoenzymes through DEAE columns and was collected in fractions. Enzyme activity in 3 separate HexB-HexA-treated mice showed increased hexosaminidase activity compared with pooled SD controls in a pattern that mirrored pooled Het control serum. These results include increased activity in fractions containing the Hex A enzyme (1–3) and the Hex B enzyme (9–12). *$p < 0.05$, **$p < 0.01$, ***$p < 0.001$, ****$p < 0.0001$.

Behavior Testing

Behavioral testing was carried out on a bi-weekly basis from the age of 8 weeks until each respective endpoint. The behavioral testing[52] used three different tests.

Mesh Test

The mesh test was used to assess muscle strength. The mouse was placed in the center of a wire mesh screen that was rotated to an inverted position over the course of 2 s, with the mouse's head declining first. The screen was then held 20 cm above a padded surface, and the time elapsed before the mouse fell off was recorded, or the test was stopped when a maximum of 60 s was reached. Each mouse was given 3 trials spaced out by 5 min, and the best trial was recorded.

Open Field Test

The OFT was used to assess overall locomotion and activity levels. The mouse was placed in a 40 cm × 40 cm arena for 5 min. Time moving, rearing activity, and distance traveled were all electronically recorded by the ActiMot system.

Righting Reflex

Righting reflex was used to assess mobility and deterioration of quality of life. The mouse was placed in the supine position, and the time elapsed until all 4 paws were on the floor surface was timed. Righting reflex was carried out 3 times on each mouse with a rest of 1 min between attempts. The longest time to righting was recorded. If a maximum score of 10 s was reached, this indicated that a humane endpoint had been reached.

Tissue and Serum Collection

Tissue samples were collected at either the designated 16-week endpoint or the long-term humane endpoint. Humane endpoints were determined by either more than 15% loss of peak body weight or an inability to right in 10 s. Euthanasia was carried out via CO_2 asphyxiation, followed by cardiac puncture, through

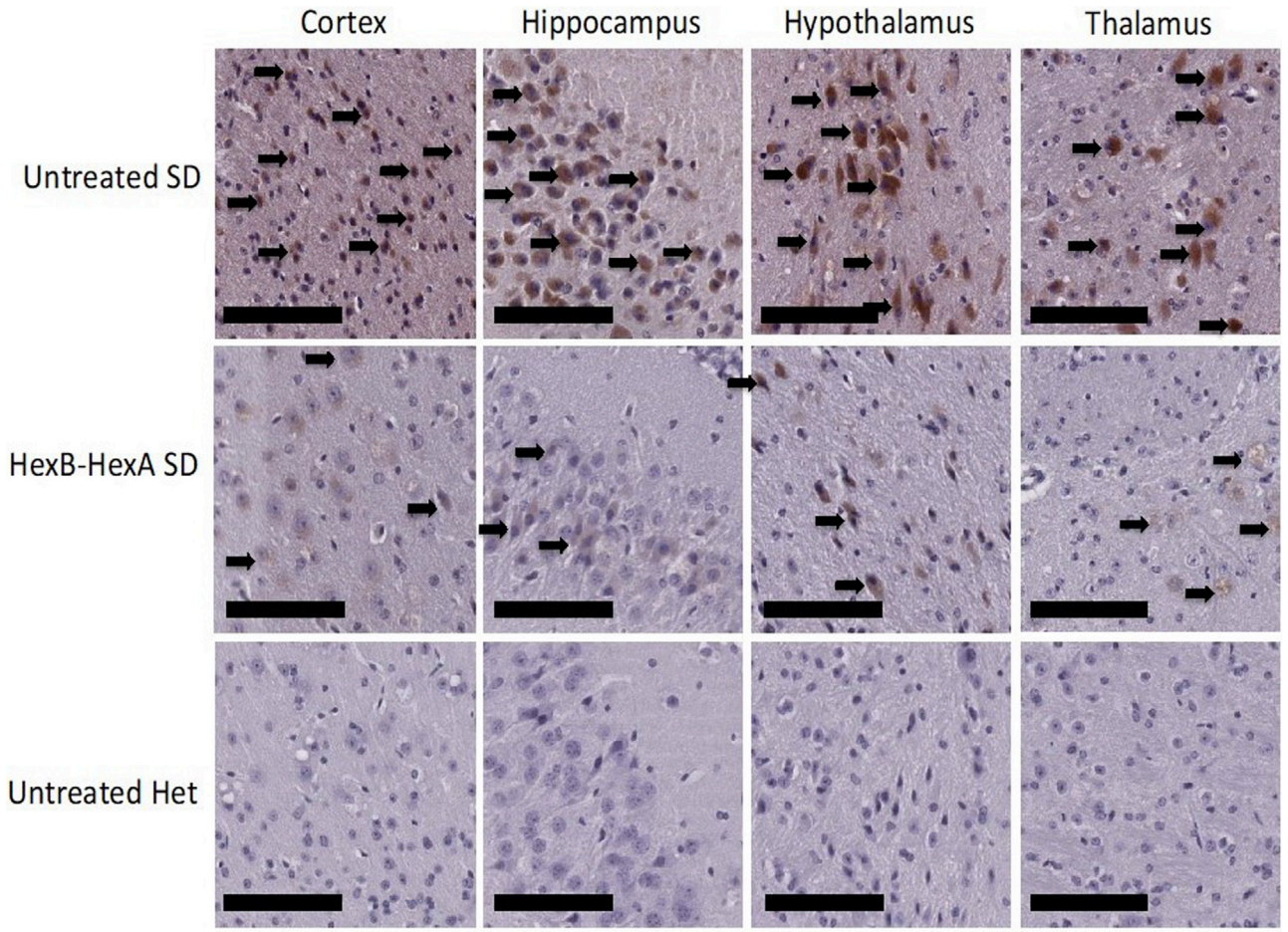

Figure 7. Histological Ganglioside Storage in Neurons of the Murine Midbrain at 16 Weeks

Shown are sections of the murine cortex, hippocampus, hypothalamus, and thalamus from SD controls, HexB-HexA-treated SD mice, and Het controls. The black arrows point to G_{M2} ganglioside-filled neurons, which were found predominately in untreated SD mice and with reduced number and severity in the HexB-HexA-treated SD mice. A reduction in storage of G_{M2} ganglioside was observed in HexB-HexA-treated mice; however, it is not a full clearance of the GM2 gangliosides. No G_{M2} ganglioside storage is observed in the Het control sections. Scale bars represent 50 μm.

which approximately 1 mL of blood was collected, and perfusion with 10 mL of chilled PBS. The whole brain was approximately divided into three parts (forebrain, midbrain, and hindbrain) using a scaled matrix tool. A 2-mm section of the midbrain was fixed in 4% paraformaldehyde overnight and then immersed in 100% ethanol until it was sent to the Queen's University Histology Department for paraffin embedding. The remaining midbrain was collected and frozen immediately for further processing.

Approximately 200 μL of serum was collected via the saphenous vein monthly starting at 8 weeks. The mice were placed in a restraining device, and hair was removed from the caudal surface of the thigh. The site was then swabbed with alcohol and covered in petroleum jelly, and a 25G needle was used to puncture the vein. Blood was collected in a capillary blood collection tube. Serum was separated from whole blood samples by centrifugation at 4,000 rpm for 10 min.

Ganglioside Storage Assays

Ganglioside extraction and visualization were performed as described previously.[53,54,56–60] Briefly, frozen midbrain sections were sonicated in 800 μL of PBS in three 10-s bursts and then centrifuged at 4°C for 20 min. 400 μL of the supernatant was taken for the hexosaminidase activity assays (described below). Gangliosides were extracted from the remaining midbrain samples using methanol and chloroform solvents. These mixed ganglioside samples were then separated on a thin-layer chromatography (TLC) plate using a 55:45:10 chloroform:methanol:0.2% calcium chloride mobile phase. Bands were visualized using orcinol in 10% sulfuric acid, and plates were dried at 120°C for 10 min. Densitometry analysis was performed, comparing the intensity of the G_{M2} ganglioside band with the total

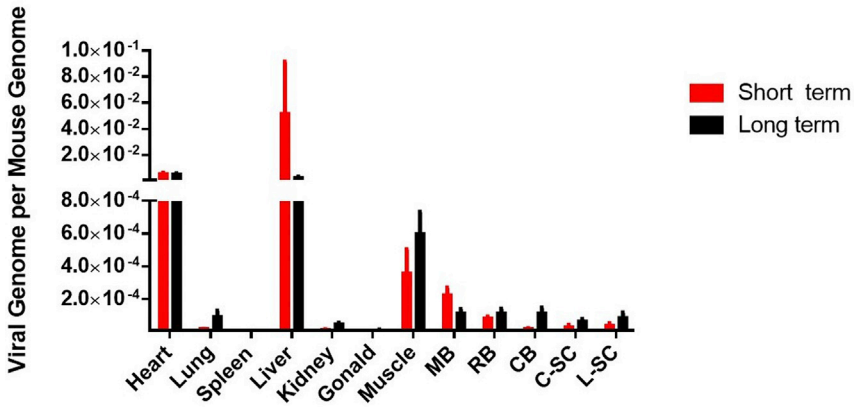

Figure 8. Vector Biodistribution of the hHEXB-P2A-HEXA Vector

Viruses were distributed in most of the organs in long-term cohort and short-term cohort mice (n = 6 each). hHexBP2AHexA was not detectable above 0.000 copies per mouse genome in mice dosed with vehicle and is not shown in the graph. Data are presented as the copies of vector DNA per diploid mouse genome found in each assessed organ.

ganglioside bands using ImageJ software. Manufactured gangliosides and SD control samples were run as the standard control on each plate.

Hexosaminidase Assays

Total hexosaminidase activity and Hex A activity was measured as described previously.[61,62] Briefly, total hexosaminidase activity was determined using the 4-methylumbelliferyl-2-acetamido-2-deoxy-β-D-glucopyranoside (4-MUG) assay, whereas the HexA enzyme activity alone was determined using the 4-MUGS assay. β-Galactosidase activity was determined using the 4-methylumbelliferyl-β-D-galactopyranoside assay as a quality control lysosomal enzyme. In all assays, the samples were incubated with the various substrates at 37°C for 1 hr. During this time, active enzyme breaks down the substrate to release a fluorescent signal. Samples were then read on the plate reader with an excitation wavelength of 365 nm and an emission wavelength of 450 nm to assess both absolute and relative levels of the signal release. Additionally, the results were compared with the 4-methylumbelliferone (4-MU) standard curve. The MB samples were diluted to 1:10 in PBS to complete the various assays; the serum samples were diluted to 1:50 in PBS.

Histology

Histological procedures were performed as described previously.[42,43] Briefly, paraffin-embedded midbrain samples were sectioned on a microtome to a thickness of 4–6 μm. Sections were then de-paraffinized in toluene for 10 min and rehydrated through 100%, 85%, and 70% EtOH for 5 min in each bath. Antigen retrieval was accomplished by heating the slides in sodium citrate antigen retrieval solution (pH 6.0) to a boil and then allowing the solution to cool at room temperature for 20 min. The slides were then blocked for both non-specific binding and endogenous peroxidase activity with 10% normal goat serum and 3% hydrogen peroxide, respectively. Overnight incubation in primary antibody and 1-hr incubation with horseradish peroxidase (HRP)-conjugated secondary antibodies were then carried out. DAB stain was then applied, followed by a hematoxylin counterstain. Slides were then dehydrated through the same series of alcohol baths in reverse order and finally in toluene for 10 min. Slides were coverslipped and visualized.

Immunohistological detection for G_{M2} ganglioside storage was accomplished with a 1:100 dilution of the chimeric murine-human immunoglobulin G1 (IgG1) anti-G_{M2} ganglioside antibody KM966 (Kyowa Hakko Kirin Co. Ltd).[63] The primary antibody was detected with an anti-human biotinylated secondary antibody at a 1:1,000 dilution.

Cell Culture and Transfection

HEKHexABKO cells were obtained from Dr. Don Mahuran at the University of Toronto. These cells express no Hex A or any other hexosaminidase activity. Cells were maintained in culture at 37°C and 5% CO_2. Cellular transfection for the DEAE protocol was carried out using a standard calcium phosphate transfection protocol. HEKHexABKO and WT HEK293 cells were grown in separate 10-cm plates. Following transfection of 1 plate of HEKHexABKO cells with the HexB-HexA-containing plasmid, cells were scraped, pelleted, and then lysed via sonication in PBS. Sonicated samples were then tested for hexosaminidase activity using the DEAE enzyme separation technique described below. Cellular transfection for the western blot protocol was conducted using Lipofectamine 2000. Cells were maintained in 6-cm plates and transfected with the HexB-HexA construct, a human HexB construct, or a GFP construct. Cell lysates were collected and lysed in radioimmunoprecipitation assay (RIPA) lysis buffer (Cell Signaling Technology, Dallas, TX; catalog number 9806).

DEAE Protocol

Cell lysates were analyzed by ion exchange chromatography on DEAE-Sepharose CL-6B (Pharmacia, NJ, USA) similarly as described previously.[64,65] Briefly, the DEAE column was pre-equilibrated with 10 mM phosphate buffer (pH 6.0) containing 5% glycerol. 500 μL of sample was loaded, followed by a wash buffer (25 mM NaCl in 10 mM NaPi [pH 6.0]), and the flowthrough was collected in 200-μL fractions (fractions 1–16). Proteins retained by the column were eluted using elution buffer 1 (200 mM NaCl in 10 mM NaPi [pH6.0]) in fractions 17–24 and elution buffer 2 (500 mM NaCl in 10 mM NaPi [pH 6.0]) in fractions 25–32. Fractions (200 μl) were collected and assayed for Hex activity with MUG substrate.

Western Blot

Clarified protein extracts were subjected to separation by SDS-PAGE and transferred to polyvinylidene fluoride (PVDF)

membranes (Millipore, Carlsbad, CA, USA; IPVH00010). 5% powdered skim milk Tris-buffered saline (TBS) solution blocked the membranes prior to probing with primary antibodies against HEXA (Abcam, Cambridge, UK; ab91624; 1:100) or HEXB (Sigma-Aldrich, St. Louis, MO, USA; SAB4501385; 1:750) and β-actin (Sigma-Aldrich, St. Louis, MO, USA; catalog number A5441; 1:750). Membranes were then subjected to 3 washes in TBS-Tween (TBS-T) divided equally in a 15-min period. Proteins of interest were detected with HRP-conjugated goat anti-mouse (Sigma-Aldrich, St. Louis, MO, USA; A5278; 1:10,000) and goat anti-rabbit (Sigma-Aldrich, St. Louis, MO, USA; A8275; 1:10,000) secondary antibodies. Visualization was conducted after repeating the wash step and utilized enhanced chemiluminescence (Bio-Rad, Hercules, CA, USA; catalog number 1705061) detection captured by exposure to scientific autoradiography film (Progene, St. Laurent, QC, Canada; catalog number 39-20810).

Vector Biodistribution

Copy numbers of the hHEXB-P2A-HEXA vector and mouse genomic DNA were determined by qPCR as reported previously. Briefly, total DNA from each organ was extracted with a gSYNC DNA extraction kit (catalog number GS100, Geneaid). All reactions were carried out using PowerUp SYBR Green Master Mix (catalog number A75242, Thermo Fisher Scientific) on an Applied Biosystems 7500 real-time PCR system following the manufacturer's instructions. For virus quantitation, plasmid DNA was used as the standard. For mouse genomic DNA quantitation, purified and quantified mouse genomic DNA was used as a standard. Primers for virus pAAV.CAG.hHexBP2AHexA.7303 ITRs4792 were as follows: forward, 5′-TATGGCAAGGGCTATGTGGT-3′; reverse, 5′-TGATTGT GTCTGGCTGAATCTT-3′. Mouse LaminB2 primers for quantitation of mouse genomic DNA were as follows: forward, 5′-GGACC CAAGGACTACCTCAAGGG-3′; reverse, 5′-AGGGCACCTCCATC TCGGAAAC-3′.

Statistics

One-way ANOVA with Bonferroni *post hoc* test was performed on the results from the ganglioside assay and the hexosaminidase assays (with the exception of the serum time courses). All of the behavioral data and the hexosaminidase serum time courses were analyzed through 2-way repeated measures ANOVA with the Bonferroni *post hoc* test. A Kaplan-Meier curve was used to assess the survival of the animals, followed by a log rank (Mantel-Cox) test. All statistical analyses were performed in GraphPad Prism 7.

AUTHOR CONTRIBUTIONS

E.W. was involved in all steps of the research, including injecting mice, monitoring behavior, and biochemical and histological analysis of samples. K.J.L.O. assisted J.S.W. with the design and production of the ssAAV9-HexB-P2A-HexA plasmid. K.J.L.O. performed cell culturing and transfection for the western blot lysates. C.R. performed and K.J.L.O. assisted with the western Blot. K.J.L.O. edited all subsequent drafts of the manuscript. Z.C. performed qPCR for the biodistribution analysis. P.T. assisted with all biochemical analyses and neonatal injections. S.J.G. produced the viral vectors. J.S.W. supervised all aspects of the project.

CONFLICTS OF INTEREST

The authors have no conflicts of interest.

ACKNOWLEDGMENTS

Funding for this research was provided by the Kingston General Hospital, Queen's University, Cure Tay-Sachs Foundation, and New Hope Research Foundation. We thank Kyowa Hakko Kirin Co., Ltd for graciously providing the KM966 antibody. Indirect administrative support for S.J.G. was provided by Research to Prevent Blindness to the UNC-CH Department of Ophthalmology.

REFERENCES

1. Gravel, R., Kaback, M.M., Proia, R.L., Sandhoff, K., and Suzuki, K. (2001). The GM2 gangliosidoses. In The Metabolic and Molecular Bases of Inherited Diseases (New York: McGraw-Hill), pp. 3827–3876.
2. Sandhoff, K., and Harzer, K. (2013). Gangliosides and gangliosidoses: principles of molecular and metabolic pathogenesis. J. Neurosci. *33*, 10195–10208.
3. Myrianthopoulos, N.C., and Aronson, S.M. (1966). Population dynamics of Tay-Sachs disease. I. Reproductive fitness and selection. Am. J. Hum. Genet. *18*, 313–327.
4. Greenberg, D.A., and Kaback, M.M. (1982). Estimation of the frequency of hexosaminidase a variant alleles in the American Jewish population. Am. J. Hum. Genet. *34*, 444–451.
5. Petersen, G.M., Rotter, J.I., Cantor, R.M., Field, L.L., Greenwald, S., Lim, J.S., Roy, C., Schoenfeld, V., Lowden, J.A., and Kaback, M.M. (1983). The Tay-Sachs disease gene in North American Jewish populations: geographic variations and origin. Am. J. Hum. Genet. *35*, 1258–1269.
6. Kaback, M., Lim-Steele, J., Dabholkar, D., Brown, D., Levy, N., and Zeiger, K.; The International TSD Data Collection Network (1993). Tay-Sachs disease–carrier screening, prenatal diagnosis, and the molecular era. An international perspective, 1970 to 1993. JAMA *270*, 2307–2315.
7. Lowden, J.A., Ives, E.J., Keene, D.L., Burton, A.L., Skomorowski, M.A., and Howard, F. (1978). Carrier detection in Sandhoff disease. Am. J. Hum. Genet. *30*, 38–45.
8. Sandhoff, K., and Christomanou, H. (1979). Biochemistry and genetics of gangliosidoses. Hum. Genet. *50*, 107–143.
9. Andermann, E., Scriver, C.R., Wolfe, L.S., Dansky, L., and Andermann, F. (1977). Genetic variants of Tay-Sachs disease: Tay-Sachs disease and Sandhoff's disease in French Canadians, juvenile Tay-Sachs disease in Lebanese Canadians, and a Tay-Sachs screening program in the French-Canadian population. Prog. Clin. Biol. Res. *18*, 161–188.
10. Der Kaloustian, V.M., Khoury, M.J., Hallal, R., Idriss, Z.H., Deeb, M.E., Wakid, N.W., and Haddad, F.S. (1981). Sandhoff disease: a prevalent form of infantile GM2 gangliosidosis in Lebanon. Am. J. Hum. Genet. *33*, 85–89.
11. Nyhan, Barshop, and Al-Aqeel. (2012a). Sandhoff Disease/GM2 gangliosidosis/deficiency of hexosaminidase A and B/hex-B subunit deficiency. In Atlas of Inherited Metabolic Disorders (London: Hodder Arnold), pp. 686–693.
12. Nyhan, Barshop, and Al-Aqeel. (2012b). Tay-Sachs disease/hexosaminidase A deficiency. In Atlas of Inherited Metabolic Disorders (London: Hodder Arnold), pp. 678–685.
13. Conzelmann, E., and Sandhoff, K. (1983-1984). Partial enzyme deficiencies: residual activities and the development of neurological disorders. Dev. Neurosci. *6*, 58–71.
14. Leinekugel, P., Michel, S., Conzelmann, E., and Sandhoff, K. (1992). Quantitative correlation between the residual activity of β-hexosaminidase A and arylsulfatase A and the severity of the resulting lysosomal storage disease. Hum. Genet. *88*, 513–523.
15. Arfi, A., Bourgoin, C., Basso, L., Emiliani, C., Tancini, B., Chigorno, V., Li, Y.T., Orlacchio, A., Poenaru, L., Sonnino, S., and Caillaud, C. (2005). Bicistronic lentiviral

vector corrects β-hexosaminidase deficiency in transduced and cross-corrected human Sandhoff fibroblasts. Neurobiol. Dis. *20*, 583–593.

16. Cardone, M. (2007). Prospects for gene therapy in inherited neurodegenerative diseases. Curr. Opin. Neurol. *20*, 151–158.

17. Foust, K.D., Nurre, E., Montgomery, C.L., Hernandez, A., Chan, C.M., and Kaspar, B.K. (2009). Intravascular AAV9 preferentially targets neonatal neurons and adult astrocytes. Nat. Biotechnol. *27*, 59–65.

18. Wang, D.B., Dayton, R.D., Henning, P.P., Cain, C.D., Zhao, L.R., Schrott, L.M., Orchard, E.A., Knight, D.S., and Klein, R.L. (2010). Expansive gene transfer in the rat CNS rapidly produces amyotrophic lateral sclerosis relevant sequelae when TDP-43 is overexpressed. Mol. Ther. *18*, 2064–2074.

19. Duque, S., Joussemet, B., Riviere, C., Marais, T., Dubreil, L., Douar, A.-M., Fyfe, J., Moullier, P., Colle, M.A., and Barkats, M. (2009). Intravenous administration of self-complementary AAV9 enables transgene delivery to adult motor neurons. Mol. Ther. *17*, 1187–1196.

20. Bevan, A.K., Duque, S., Foust, K.D., Morales, P.R., Braun, L., Schmelzer, L., Chan, C.M., McCrate, M., Chicoine, L.G., Coley, B.D., et al. (2011). Systemic gene delivery in large species for targeting spinal cord, brain, and peripheral tissues for pediatric disorders. Mol. Ther. *19*, 1971–1980.

21. Gray, S.J., Matagne, V., Bachaboina, L., Yadav, S., Ojeda, S.R., and Samulski, R.J. (2011). Preclinical differences of intravascular AAV9 delivery to neurons and glia: a comparative study of adult mice and nonhuman primates. Mol. Ther. *19*, 1058–1069.

22. Dehay, B., Dalkara, D., Dovero, S., Li, Q., and Bezard, E. (2012). Systemic scAAV9 variant mediates brain transduction in newborn rhesus macaques. Sci. Rep. *2*, 253.

23. Mattar, C.N., Waddington, S.N., Biswas, A., Johana, N., Ng, X.W., Fisk, A.S., Fisk, N.M., Tan, L.G., Rahim, A.A., Buckley, S.M., et al. (2013). Systemic delivery of scAAV9 in fetal macaques facilitates neuronal transduction of the central and peripheral nervous systems. Gene Ther. *20*, 69–83.

24. Akli, S., Guidotti, J.E., Vigne, E., Perricaudet, M., Sandhoff, K., Kahn, A., and Poenaru, L. (1996). Restoration of hexosaminidase A activity in human Tay-Sachs fibroblasts via adenoviral vector-mediated gene transfer. Gene Ther. *3*, 769–774.

25. Guidotti, J.E., Mignon, A., Haase, G., Caillaud, C., McDonell, N., Kahn, A., and Poenaru, L. (1999). Adenoviral gene therapy of the Tay-Sachs disease in hexosaminidase A-deficient knock-out mice. Hum. Mol. Genet. *8*, 831–838.

26. Itakura, T., Kuroki, A., Ishibashi, Y., Tsuji, D., Kawashita, E., Higashine, Y., Sakuraba, H., Yamanaka, S., and Itoh, K. (2006). Inefficiency in GM2 ganglioside elimination by human lysosomal beta-hexosaminidase beta-subunit gene transfer to fibroblastic cell line derived from Sandhoff disease model mice. Biol. Pharm. Bull. *29*, 1564–1569.

27. Yamanaka, S., Johnson, M.D., Grinberg, A., Westphal, H., Crawley, J.N., Taniike, M., Suzuki, K., and Proia, R.L. (1994). Targeted disruption of the Hexa gene results in mice with biochemical and pathologic features of Tay-Sachs disease. Proc. Natl. Acad. Sci. USA *91*, 9975–9979.

28. Sango, K., Yamanaka, S., Hoffmann, A., Okuda, Y., Grinberg, A., Westphal, H., McDonald, M.P., Crawley, J.N., Sandhoff, K., Suzuki, K., and Proia, R.L. (1995). Mouse models of Tay-Sachs and Sandhoff diseases differ in neurologic phenotype and ganglioside metabolism. Nat. Genet. *11*, 170–176.

29. Phaneuf, D., Wakamatsu, N., Huang, J.Q., Borowski, A., Peterson, A.C., Fortunato, S.R., Ritter, G., Igdoura, S.A., Morales, C.R., Benoit, G., et al. (1996). Dramatically different phenotypes in mouse models of human Tay-Sachs and Sandhoff diseases. Hum. Mol. Genet. *5*, 1–14.

30. Cohen-Tannoudji, M., Marchand, P., Akli, S., Sheardown, S.A., Puech, J.P., Kress, C., Gressens, P., Nassogne, M.C., Beccari, T., Muggleton-Harris, A.L., et al. (1995). Disruption of murine Hexa gene leads to enzymatic deficiency and to neuronal lysosomal storage, similar to that observed in Tay-Sachs disease. Mamm. Genome *6*, 844–849.

31. Huang, J.Q., Trasler, J.M., Igdoura, S., Michaud, J., Hanal, N., and Gravel, R.A. (1997). Apoptotic cell death in mouse models of GM2 gangliosidosis and observations on human Tay-Sachs and Sandhoff diseases. Hum. Mol. Genet. *6*, 1879–1885.

32. Lawson, C.A., and Martin, D.R. (2016). Animal models of GM2 gangliosidosis: utility and limitations. Appl. Clin. Genet. *9*, 111–120.

33. Bourgoin, C., Emiliani, C., Kremer, E.J., Gelot, A., Tancini, B., Gravel, R.A., Drugan, C., Orlacchio, A., Poenaru, L., and Caillaud, C. (2003). Widespread distribution of beta-hexosaminidase activity in the brain of a Sandhoff mouse model after coinjection of adenoviral vector and mannitol. Gene Ther. *10*, 1841–1849.

34. Cachón-González, M.B., Wang, S.Z., Lynch, A., Ziegler, R., Cheng, S.H., and Cox, T.M. (2006). Effective gene therapy in an authentic model of Tay-Sachs-related diseases. Proc. Natl. Acad. Sci. USA *103*, 10373–10378.

35. Cachón-González, M.-B., Wang, S.Z., Ziegler, R., Cheng, S.H., and Cox, T.M. (2014). Reversibility of neuropathology in Tay-Sachs-related diseases. Hum. Mol. Genet. *23*, 730–748.

36. Bradbury, A.M., Cochran, J.N., McCurdy, V.J., Johnson, A.K., Brunson, B.L., Gray-Edwards, H., Leroy, S.G., Hwang, M., Randle, A.N., Jackson, L.S., et al. (2013). Therapeutic response in feline sandhoff disease despite immunity to intracranial gene therapy. Mol. Ther. *21*, 1306–1315.

37. Martino, S., Marconi, P., Tancini, B., Dolcetta, D., De Angelis, M.G.C., Montanucci, P., Bregola, G., Sandhoff, K., Bordignon, C., Emiliani, C., et al. (2005). A direct gene transfer strategy via brain internal capsule reverses the biochemical defect in Tay-Sachs disease. Hum. Mol. Genet. *14*, 2113–2123.

38. McCurdy, V.J., Rockwell, H.E., Arthur, J.R., Bradbury, A.M., Johnson, A.K., Randle, A.N., Brunson, B.L., Hwang, M., Gray-Edwards, H.L., Morrison, N.E., et al. (2015). Widespread correction of central nervous system disease after intracranial gene therapy in a feline model of Sandhoff disease. Gene Ther. *22*, 181–189.

39. Rockwell, H.E., McCurdy, V.J., Eaton, S.C., Wilson, D.U., Johnson, A.K., Randle, A.N., Bradbury, A.M., Gray-Edwards, H.L., Baker, H.J., Hudson, J.A., et al. (2015). AAV-mediated gene delivery in a feline model of Sandhoff disease corrects lysosomal storage in the central nervous system. ASN Neuro *7*, 1759091415569908.

40. Gray-Edwards, H.L., Brunson, B.L., Holland, M., Hespel, A.-M., Bradbury, A.M., McCurdy, V.J., Beadlescomb, P.M., Randle, A.N., Salibi, N., Denney, T.S., et al. (2015). Mucopolysaccharidosis-like phenotype in feline Sandhoff disease and partial correction after AAV gene therapy. Mol. Genet. Metab. *116*, 80–87.

41. Sargeant, T.J., Wang, S., Bradley, J., Smith, N.J.C., Raha, A.A., McNair, R., Ziegler, R.J., Cheng, S.H., Cox, T.M., and Cachón-González, M.B. (2011). Adeno-associated virus-mediated expression of β-hexosaminidase prevents neuronal loss in the Sandhoff mouse brain. Hum. Mol. Genet. *20*, 4371–4380.

42. Walia, J.S., Altaleb, N., Bello, A., Kruck, C., LaFave, M.C., Varshney, G.K., Burgess, S.M., Chowdhury, B., Hurlbut, D., Hemming, R., et al. (2015). Long-term correction of Sandhoff disease following intravenous delivery of rAAV9 to mouse neonates. Mol. Ther. *23*, 414–422.

43. Osmon, K.J., Woodley, E., Thompson, P., Ong, K., Karumuthil-Melethil, S., Keimel, J.G., et al. (2016). Systemic Gene Transfer of a Hexosaminidase Variant Using a scAAV9.47 Vector Corrects GM2 Gangliosidosis in Sandhoff Mice. Hum. Gene Ther. *27*, 497–508.

44. Kyrkanides, S., Miller, J.H., Brouxhon, S.M., Olschowka, J.A., and Federoff, H.J. (2005). beta-hexosaminidase lentiviral vectors: transfer into the CNS via systemic administration. Brain Res. Mol. Brain Res. *133*, 286–298.

45. Rastall, D.P., and Amalfitano, A. (2015). Recent advances in gene therapy for lysosomal storage disorders. Appl. Clin. Genet. *8*, 157–169.

46. Kim, J.H., Lee, S.-R., Li, L.-H., Park, H.-J., Park, J.-H., Lee, K.Y., Kim, M.K., Shin, B.A., and Choi, S.Y. (2011). High cleavage efficiency of a 2A peptide derived from porcine teschovirus-1 in human cell lines, zebrafish and mice. PLoS ONE *6*, e18556.

47. Tang, W., Ehrlich, I., Wolff, S.B.E., Michalski, A.M., Wölfl, S., Hasan, M.T., Lüthi, A., and Sprengel, R. (2009). Faithful expression of multiple proteins via 2A-peptide self-processing: a versatile and reliable method for manipulating brain circuits. J. Neurosci. *29*, 8621–8629.

48. Wang, Y., Wang, F., Wang, R., Zhao, P., and Xia, Q. (2015). 2A self-cleaving peptide-based multi-gene expression system in the silkworm Bombyx mori. Sci. Rep. *5*, 16273.

49. Liu, Z., Chen, O., Wall, J.B.J., Zheng, M., Zhou, Y., Wang, L., Ruth Vaseghi, H., Qian, L., and Liu, J. (2017). Systematic comparison of 2A peptides for cloning multi-genes in a polycistronic vector. Sci. Rep. *7*, 2193.

50. Tropak, M.B., Yonekawa, S., Karumuthil-Melethil, S., Thompson, P., Wakarchuk, W., Gray, S.J., Walia, J.S., Mark, B.L., and Mahuran, D. (2016). Construction of a hybrid β-hexosaminidase subunit capable of forming stable homodimers that hydrolyze GM2 ganglioside in vivo. Mol. Ther. Methods Clin. Dev. *3*, 15057.

51. Wu, Y.-P., and Proia, R.L. (2004). Deletion of macrophage-inflammatory protein 1 alpha retards neurodegeneration in Sandhoff disease mice. Proc. Natl. Acad. Sci. USA *101*, 8425–8430.

52. Deacon, R.M.J. (2013). Measuring the Strength of Mice. J. Vis. Exp. *76*, 2610.

53. Gray, S.J., Blake, B.L., Criswell, H.E., Nicolson, S.C., Samulski, R.J., McCown, T.J., and Li, W. (2010). Directed evolution of a novel adeno-associated virus (AAV) vector that crosses the seizure-compromised blood-brain barrier (BBB). Mol. Ther. *18*, 570–578.

54. Cachón-González, M.B., Wang, S.Z., McNair, R., Bradley, J., Lunn, D., Ziegler, R., Cheng, S.H., and Cox, T.M. (2012). Gene transfer corrects acute GM2 gangliosidosis–potential therapeutic contribution of perivascular enzyme flow. Mol. Ther. *20*, 1489–1500.

55. Arber, C., Abhyankar, H., Heslop, H.E., Brenner, M.K., Liu, H., Dotti, G., and Savoldo, B. (2013). The immunogenicity of virus-derived 2A sequences in immunocompetent individuals. Gene Ther. *20*, 958–962.

56. Gray, S.J., Nagabhushan Kalburgi, S., McCown, T.J., and Jude Samulski, R. (2013). Global CNS gene delivery and evasion of anti-AAV-neutralizing antibodies by intrathecal AAV administration in non-human primates. Gene Ther. *20*, 450–459.

57. Folch, J., Ascoli, I., Lees, M., Meath, J.A., and LeBARON, N. (1951). Preparation of lipide extracts from brain tissue. J. Biol. Chem. *191*, 833–841.

58. Folch, J., Lees, M., and Sloane Stanley, G.H. (1957). A simple method for the isolation and purification of total lipides from animal tissues. J. Biol. Chem. *226*, 497–509.

59. Wherrett, J.R., and Cumings, N.J. (1963). Detection and resolution of gangliosides in lipid extracts by thin-layer chromatography. Biochem. J. *86*, 378–382.

60. Tropak, M.B., Bukovac, S.W., Rigat, B.A., Yonekawa, S., Wakarchuk, W., and Mahuran, D.J. (2010). A sensitive fluorescence-based assay for monitoring GM2 ganglioside hydrolysis in live patient cells and their lysates. Glycobiology *20*, 356–365.

61. Tropak, M.B., Reid, S.P., Guiral, M., Withers, S.G., and Mahuran, D. (2004). Pharmacological enhancement of β-hexosaminidase activity in fibroblasts from adult Tay-Sachs and Sandhoff Patients. J. Biol. Chem. *279*, 13478–13487.

62. Maegawa, G.H.B., Tropak, M., Buttner, J., Stockley, T., Kok, F., Clarke, J.T.R., and Mahuran, D.J. (2007). Pyrimethamine as a potential pharmacological chaperone for late-onset forms of GM2 gangliosidosis. J. Biol. Chem. *282*, 9150–9161.

63. Yamada, T., Bando, H., Takeuchi, S., Kita, K., Li, Q., Wang, W., Akinaga, S., Nishioka, Y., Sone, S., and Yano, S. (2011). Genetically engineered humanized anti-ganglioside GM2 antibody against multiple organ metastasis produced by GM2-expressing small-cell lung cancer cells. Cancer Sci. *102*, 2157–2163.

64. Martino, S., Emiliani, C., Orlacchio, A., Hosseini, R., and Stirling, J.L. (1995). Beta-N-acetylhexosaminidases A and S have similar sub-cellular distributions in HL-60 cells. Biochim. Biophys. Acta *1243*, 489–495.

65. Sinici, I., Yonekawa, S., Tkachyova, I., Gray, S.J., Samulski, R.J., Wakarchuk, W., Mark, B.L., and Mahuran, D.J. (2013). In cellulo examination of a beta-alpha hybrid construct of beta-hexosaminidase A subunits, reported to interact with the GM2 activator protein and hydrolyze GM2 ganglioside. PLoS ONE *8*, e57908.